*17th World Conference on Earthquake Engineering, 17WCEE*
*Sendai, Japan - September 13th to 18th 2020*

# DEVELPOMENT OF ESTIMATION METHOD OF BUILDING INPUT GROUND MOTIONS USING SEISMIC RECORDS ON SHM AND MeSO-net

K. Hasegawa(1), A. Kusaka(2), K. Kanda (3), T. Kimura (4) , S. Sakai (5)

(1) *Deputy Manager, Kobori Research Complex Inc., Tokyo, Japan, hasegkan@kobori-takken.co.jp*
(2) *Deputy General Manager, Kobori Research Complex Inc., Tokyo, Japan*
(3) *Principal Researcher, Kobori Research Complex Inc., Tokyo, Japan*
(4) *Chief Researcher, National Research Institute for Earth Science and Disaster Resilience, Tsukuba, Japan*
(5) *Associate Professor, Earthquake Research Institute, University of Tokyo, Tokyo, Japan*

## *Abstract*

This paper proposes a method to estimate input ground motions to buildings rapidly and accurately after an earthquake using the seismic records on Metropolitan Seismic Observation network (MeSO-net) by the event.

In Japan, huge population and great numbers of buildings and companies are concentrated in Tokyo metropolitan area. When strong earthquake hit this area, a great number of buildings will be damaged and the first responders such as construction companies will have to survey and assess safety of the buildings for resuming social activities. However, the number of the engineers is insufficient. It is important to decide the priority of buildings and dispatch engineers efficiently. For deciding this priority, one of the most important information is possibility of damage to individual buildings. To accurately estimate the possibility of damage to individual buildings, the estimation accuracy of the input ground motions to individual buildings should be improved.

One idea to improve the estimation accuracy of the building input ground motions is using seismic records of dense seismic observation array such as MeSO-net. In MeSO-net, approximately 300 accelerometers are installed at intervals of several kilometers in Tokyo metropolitan area at 20 meters underground. To estimate the input ground motions based on the seismic records of MeSO-net, the effect of soil amplification and soil-structure interaction should be evaluated quantitatively. To evaluate this effect, the records of building input ground motions are also required. Recently in Japan, the number of seismic instrumented building is increasing for the purpose of structural health monitoring or the like. On most of instrumented buildings, responses of their ground floor and/or underground floor are measured.

In this paper, the observed records of 81 instrumented buildings are subjected which are recorded on the ground floor or underground floor and regarded as building input ground motions. The buildings are located in Tokyo metropolitan area. 2,487 acceleration records are obtained by 137 earthquake during the period of April, 2015 to March, 2018. The relationships between the records of the buildings and the nearest MeSO-net stations are statistically analyzed by acceleration response spectrum. As a result, it is found that the building input ground motion around individual MeSO-net station can be estimated utilizing the records of the buildings around the MeSO-net station.

*Keywords: structural health monitoring; MeSO-net; building input ground motion;*

 



## 1. Introduction

In Japan, huge population and great numbers of buildings and companies are concentrated in Tokyo metropolitan area. When strong earthquake hit this area, a great number of damaged buildings will occur and the first responders such as construction companies will have to survey and assess safety of the buildings for resuming social activities. However, the number of the engineers is limited and insufficient. It is important to decide the priority of buildings and dispatch engineers efficiently. For deciding this priority, one of the most important information is possibility of damage to individual buildings. To accurately estimate the possibility of damage to individual buildings, the estimation accuracy of the input ground motions to individual buildings should be improved.

One idea to improve the estimation accuracy of the building input ground motions is using seismic records of dense seismic observation array such as Metropolitan Seismic Observation network (MeSO-net). In MeSO-net, approximately 300 accelerometers are installed at intervals of several kilometers in Tokyo metropolitan area at 20 meters underground [1]. To estimate the input ground motions based on the seismic records of MeSO-net, the effect of soil amplification and soil-structure interaction should be evaluated quantitatively. To evaluate this effect, the records of building input ground motions are also required. Recently in Japan, the number of seismic instrumented building is increasing for the purpose of structural health monitoring or the like. On most of instrumented buildings, responses of their ground floor and/or underground floor are measured and they can be regarded as building input ground motions.

In this paper, the estimation method of building input ground motions is discussed on the basis of seismic records on instrumented buildings and MeSO-net. In the analysis, 2,487 seismic records on 81 buildings are collected which are recorded on the ground floor or underground floor and regarded as building input ground motions. The relationships between the records of the buildings and the nearest MeSO-net stations are statistically analyzed by acceleration response spectrum.

## 2. Estimation method of building input ground motions

Figure 1 shows the overview of the discussed estimation method of building input ground motions using the seismic records on MeSO-net by the earthquake event.

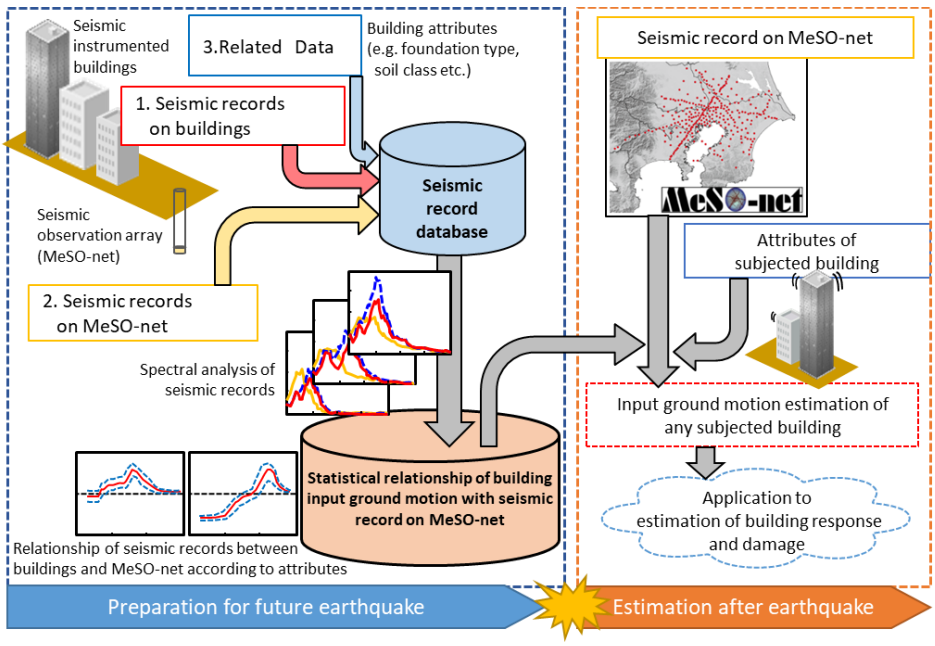


Fig. 1 – Overview of the discussed estimation method of building input ground motions



 



In preparation for future strong earthquake, statistical relationships are calculated between building input ground motion and seismic record on MeSO-net. For this statistical calculation, the seismic record database is constructed. This database contains pairs of seismic records on instrumented buildings and their nearest MeSO-net stations by same earthquake events. Also, this database contains building attributes of these instrumented buildings (e.g. foundation type, soil class etc.).

In the future, the input ground motion can be estimated for any subjected building using seismic records on MeSO-net, prepared statistical relationships and attribute information of subjected building. This estimated input ground motion will be able to apply to estimate their building response and damage after an earthquake event.

## 3. Construction of seismic record database

Figure 2 shows the overview of the construction workflow of seismic record database. In this paper, seismic records are collected which is recorded on buildings and nearest MeSO-net stations by 137 earthquake events that occurred from April 2015 to March 2018. Figure 3 shows distribution of epicenters of subjected earthquake events and Fig. 4 shows distribution of subjected instrumented buildings and nearest MeSO-net stations. The following subsections deal with each collected data in this database.

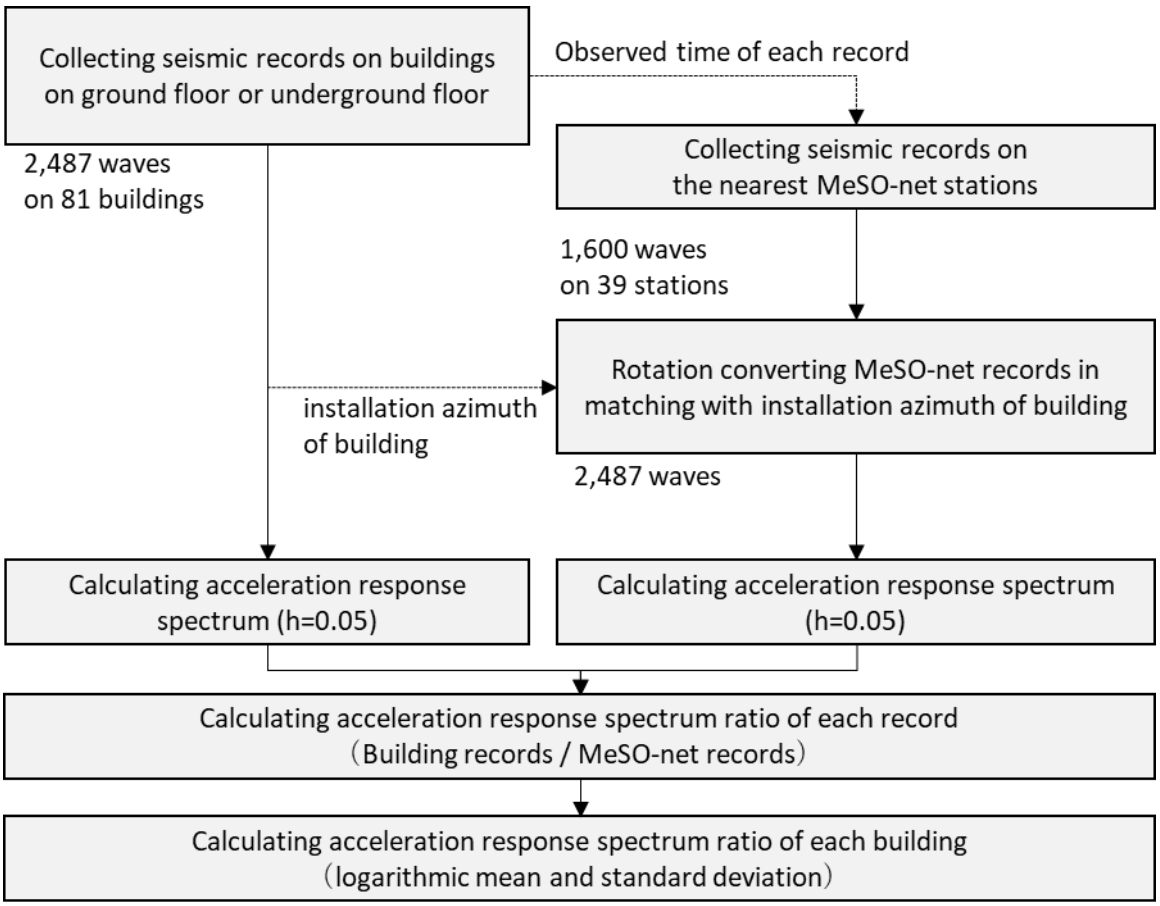


Fig. 2 – Overview of the construction workflow of seismic record database



 



## 3.1 Seismic records on buildings

In this paper, 81 instrumented buildings are subjected to collect seismic records. These buildings are distributed in 80 kilometers square as shown in Fig. 4 which is almost overlap the area the MeSO-net stations are distributed. These all buildings are non-wooden buildings. Most of them are office buildings and some of them have other occupancy such as commercial buildings. Figure 5 shows distribution of number of stories above ground and foundation type of these buildings.

On some floor of each building, three-axis accelerometers are instrumented in purpose of post-earthquake damage evaluation. In this paper, seismic records recorded on ground floor or underground floor in each building are collected and regarded as building input ground motions. Figure 6 shows distribution of number of records of each building. The numbers of records vary by building. It is because records are stored only when they exceed trigger value and some buildings began to be observed during the data collection period. 2,487 acceleration records are collected by 137 earthquake.

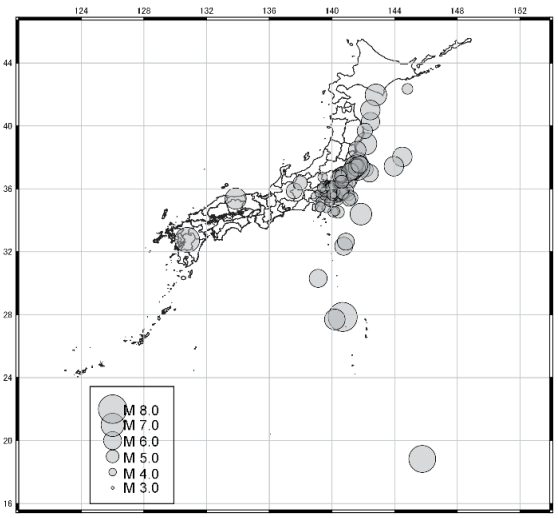


Fig. 3 – Epicenter distribution map

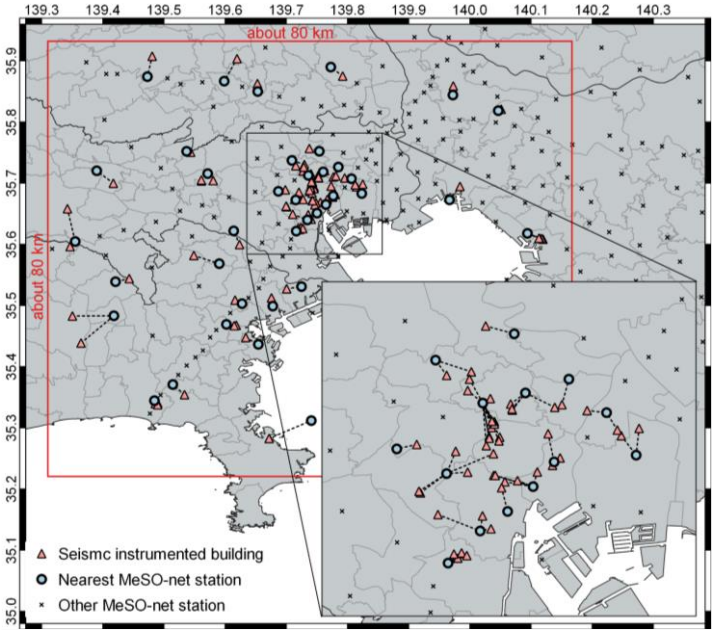


Fig. 4 – Observation point distribution map

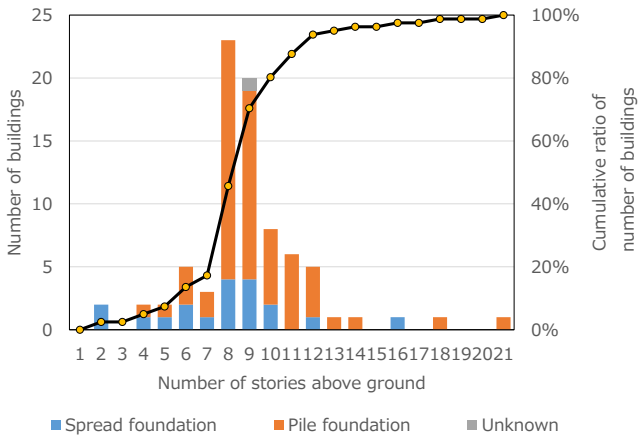


Fig. 5 – Distribution of stories and foundation type

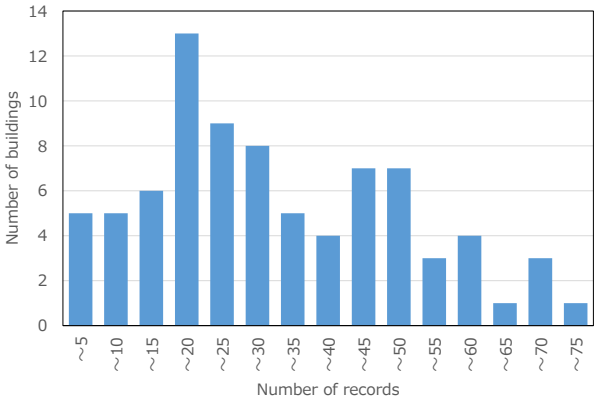


Fig. 6 – Distribution of number of records



 



### 3.2 Seismic records on MeSO-net

For comparison with building records, two horizontal acceleration records are collected recorded on the nearest MeSO-net stations of the subjected buildings. MeSO-net system records observations 24-hour continuously, so we cut out and collected the MeSO-net records so as to envelop the recording time of the seismic records on referring buildings. In densely populated areas, multiple buildings refer to the same MeSO-net station, so a total of 1,600 acceleration records are collected at 39 MeSO-net stations, which are fewer than buildings.

MeSO-net records are rotation converted in matching with installation azimuth of referring buildings from installation azimuth of the MeSO-net accelerometers [2]. After the rotation conversion, acceleration response spectrum (h = 0.05) of the seismic records on buildings and MeSO-net are calculated.

### 3.3 Related data

For analysis of the records dealed in subsections 3.1 and 3.2, attributes of each building and MeSO-net station are collected from design documents, seismic diagnosis reports, and other public information. Table 1 shows examples of items of the collected attributes. Engineering geomorphologic classification and Vs30 are values of grid cells of 7.5 arc-seconds in latitude × 11.25 arc-seconds of each building and MeSO-net station located which are downloaded from J-SHIS [3].

Table 1 – Examples of items of the collected attributes

| | | |
|---|---|---|
| Building | Outline | Constructed year, Total floor area, Building structure, Height, Number of stories above / below the ground, Fundamental period in design |
| | Foundation outline | Foundation type, Foundation bed depth, Foundation perimeter length, Foundation area, Pile type, Pile diameter, Pile length, Number of piles |
| | Soil information | Engineering geomorphologic classification, Vs30, Soil class, Presence of geological column |
| MeSO-net | Soil information | Engineering geomorphologic classification, Vs30 |

## 4. Acceleration response spectrum ratio of each building

### 4.1 Calculation of acceleration response spectrum ratio

First of all, we calculate $\mathrm{SaR}_{i,k,(x,y)}(T)$ that are acceleration response spectrum ratios of the building records to the referred MeSO-net records in each horizontal direction of building records. Here, $i$ is building number (1 to 81), $k$ is consecutive record number of building $i$ and $x$ and $y$ are 2 horizontal directions of building records. The logarithmic mean $\mu_{i,(x,y)}(T)$ and logarithmic standard deviation $\sigma_{i,(x,y)}(T)$ of each direction of each building are calculated. Since $\mu_{i,(x,y)}(T)$ are confirmed to be similar regardless of the direction $x$ and $y$ in each building, $\mathrm{SaR}_{i,k,(x,y)}(T)$ are tabulated without dividing the direction $x$ and $y$, and the logarithmic mean $\mu_i(T)$and logarithmic standard deviation $\sigma_i(T)$ of each building $i$ are calculated by Eq.(1).

$$\begin{cases} \mu_i(T) = \dfrac{1}{2n_{e,i}} \displaystyle\sum_{k=1}^{n_{e,i}} \left\{ \ln(\mathrm{SaR}_{i,k,x}(T)) + \ln(\mathrm{SaR}_{i,k,y}(T)) \right\} \\ {\sigma_i}^2(T) = \dfrac{1}{2n_{e,i}-1} \displaystyle\sum_{k=1}^{n_{e,i}} \left\{ \ln(\mathrm{SaR}_{i,k,x}(T)) + \ln(\mathrm{SaR}_{i,k,y}(T)) - 2\mu_i(T) \right\}^2 \end{cases} \quad (1)$$

Hear, $n_{e,i}$ is number of records of the building $i$. Figure 7 shows $\mathrm{SaR}_{i,k,(x,y)}(T)$, $\mu_i(T)$, and $\sigma_i(T)$ of 3 example buildings. $\mu_i(T)$ of Building 1 and 2 are looks similar because they are located nearby, the same



 



number of basement floor and referring to the same MeSO-net station. In contrast, Building 3 is an example building which have deep basement and reffering to the other MeSO-net station.

**Building 1**

| Attribute | |
|---|---|
| Structure | SRC |
| No. Stories | 11 / B1 |
| Fund. Type | Pile |
| Observed Floor | 1st floor |
| Referred MeSO-net | E.KHDM |
| Dist. from MeSO-net | 2.34 km |
| No. records | 70 |

**Building 2**

| Attribute | |
|---|---|
| Structure | SRC |
| No.Stories | 8/ B1 |
| Fund.Type | Pile |
| Observed Floor | 1st floor |
| Referred MeSO-net | E.KHDM |
| Dist. from MeSO-net | 2.41 km |
| No. records | 50 |

**Building 3**

| Attribute | |
|---|---|
| Structure | S |
| No.Stories | 11/ B5 |
| Fund.Type | Pile |
| Observed Floor | 1st floor |
| Referred MeSO-net | E.YKKM |
| Dist. from MeSO-net | 1.21 km |
| No. records | 8 |

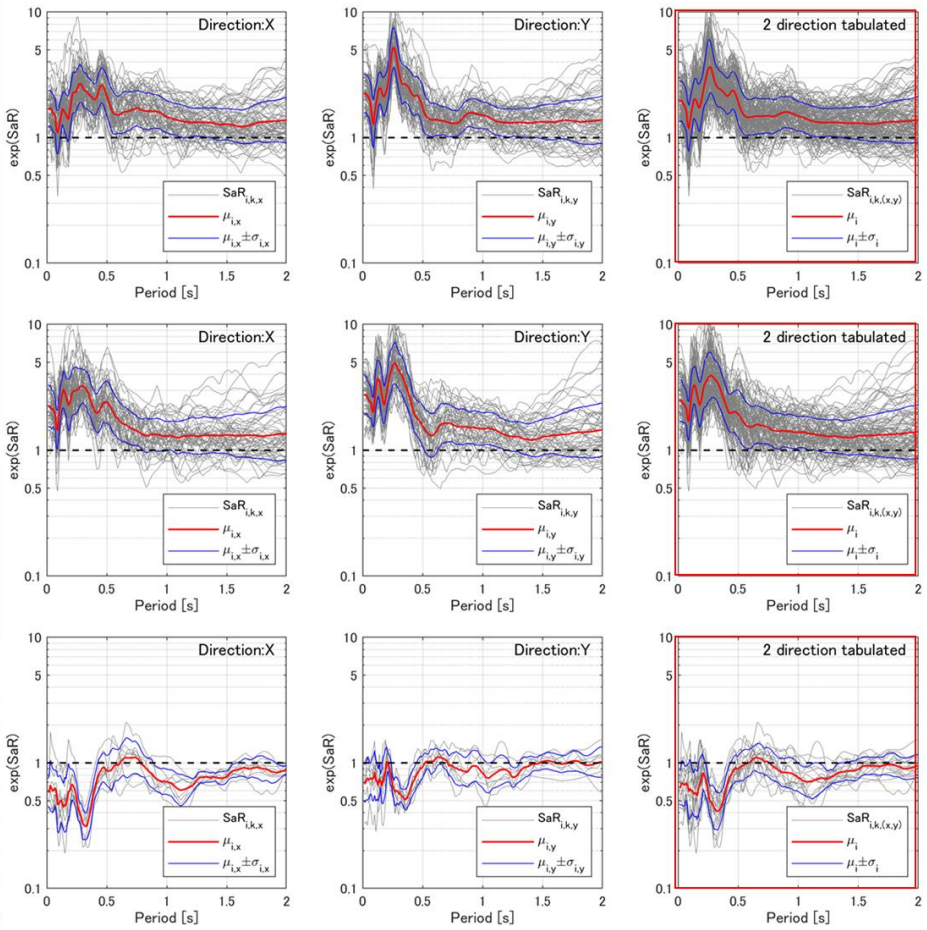


Fig. 7 – Acceleration response spectrum ratios of example buildings

## 4.2 Variation of acceleration response spectrum ratio

Figure 8 shows relationship between $\sigma_i(T = 1.0s)$ and distance between observation points (i.e. distance between each building and referred MeSO-net station). As Fig. 8 shows, it is confirmed that $\sigma_i(T)$ and the distances between observation points are related to positive correlation.

For comparison of the referred seismic observation array, seismic records are collected which are recorded on ground surface of nearest station of Kyoshin Net (K-net) or Kiban-Kyoshin Net (KiK-net) [4] of each building. By the same method in case of referring MeSO-net records, $\mu_i^K(T)$ and $\sigma_i^K(T)$ of each building are calculated that are logarithmic mean and standard deviation of the acceleration response spectrum ratios in case of referring nearest K-net/ KiK-net stations. Figure 9 shows distribution of distance from each building to nearest MeSO-net or K-net / KiK-net stations and Fig. 10 shows relationship between $\sigma_i, \sigma_i^K\ (T = 1.0s)$ and distance between observation points. Positive correlation is inferred between variation of acceleration response spectrum ratios and the distances between observation points regardless of references to MeSO-net or K-net / KiK-net. It suggests the effectiveness to refer to a dense seismic observation array such as MeSO-net for the purpose of estimating input ground motions.



 



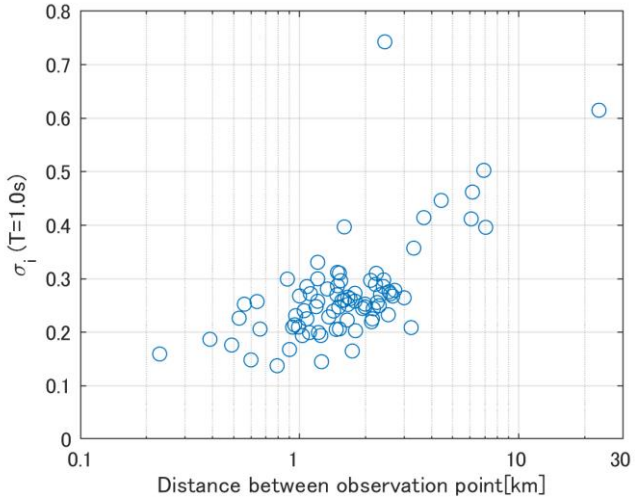


Fig. 8 – Relationship between $\sigma_i(1.0s)$ and distance from referred MeSO-net station

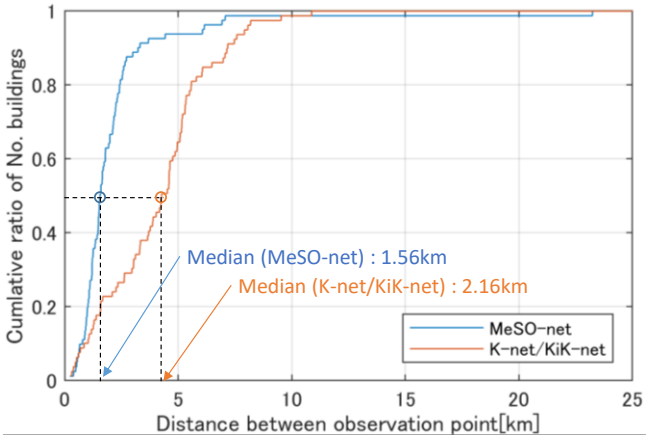


Fig. 9 – Distribution of distances between observation points

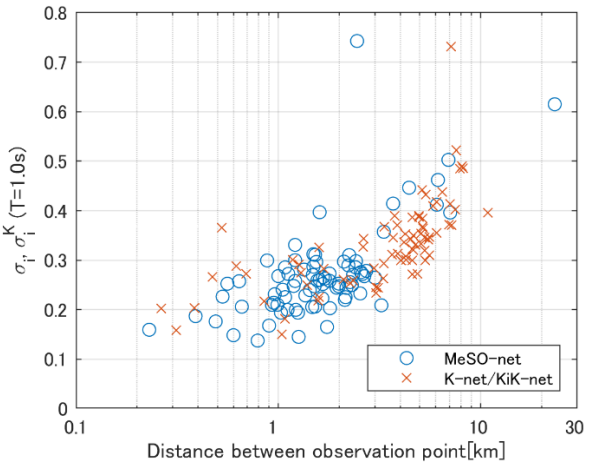


Fig. 10 – Relationship between $\sigma_i, \sigma_i^K$ $(T = 1.0s)$ and distances between observation points

## 4.3 Determinative attribute of acceleration response spectrum ratio

In order to search which attribute affects strongly to the acceleration response spectrum ratio $\mu_i(T)$, hierarchical clustering is performed by the Ward's method[5] . For this clustering, 10 points of $\mu_i(T)$ are extracted at logarithmic intervals of periods in 0.2s ≤ T ≤1.5s. Fig. 11 shows the result of classifying $\mu_i(T)$ of 81 buildings into 4 clusters.

As a result of checking attributes of the buildings belonging to each cluster, it was confirmed that buildings referring to the same MeSO-net station tended to be classified into the same cluster. There are two possible reasons. One is that $\mu_i(T)$ are strongly influenced by the soil characteristic of MeSO-net stations. The other is that the buildings referring to the same MeSO-net station tend to have similar characteristic of soil and building because of geographical closeness.



 



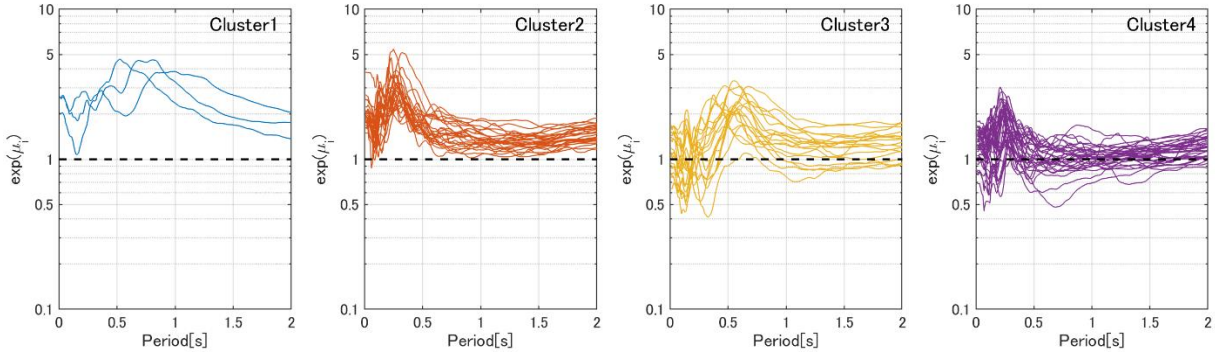


Fig. 11 – Classified $\mu_i(T)$ into 4 clusters

## 5. Acceleration response spectrum ratio of buildings referring same MeSO-net

In order to compare buildings referring to the same MeSO-net station, buildings referring same MeSO-net station are grouped. Then mean acceleration response spectrum ratio $\overline{\mu_j}(T)$ and standard deviation $\overline{\sigma_j}(T)$ are calculated for building groups by Eq.(2).

$$\begin{cases} \overline{\mu_j}(T) = \dfrac{1}{n_{b,j}} \displaystyle\sum_{k=1}^{n_{b,j}} \mu_k(T) \\ \overline{\sigma_j}^2(T) = \dfrac{1}{n_{b,j}} \displaystyle\sum_{k=1}^{n_{b,j}} {\sigma_k}^2(T) + \dfrac{1}{n-1} \displaystyle\sum_{k=1}^{n_{b,j}} \left(\mu_k(T) - \overline{\mu_j}(T)\right)^2 \\ \qquad = \quad \overline{\sigma_{\mathrm{E},j}}^2(T) + \overline{\sigma_{\mathrm{B},j}}^2(T) \end{cases} \tag{2}$$

Here, $j$ is the referred MeSO-net station, $n_{b,j}$ is the number of building referring to MeSO-net station $j$ and $(\mu_k, \sigma_k)$ is $(\mu_i, \sigma_i)$ of each building referring to MeSO-net station $j$ $(1 \le k \le n_{b,j})$. For this calculation, the buildings are subjected which have more than 5 records and located within 5 km from referring MeSO-net stations. The number of MeSO-net stations referred by multiple buildings are 14.

As Eq. (2), $\overline{\sigma_j}^2(T)$ is determined by $\overline{\sigma_{\mathrm{E},j}}^2(T)$ and $\overline{\sigma_{\mathrm{B},j}}^2(T)$. $\overline{\sigma_{\mathrm{E},j}}^2(T)$ means average of the variation between seismic records of each building and $\overline{\sigma_{\mathrm{B},j}}^2(T)$ means variation between $\mu_k(T)$ of buildings. Figures 12 and 13 show examples of $\mu_k(T)$, $\overline{\mu_j}(T)$ , $\overline{\sigma_j}(T)$ and $\overline{\sigma_{\mathrm{E},j}}(T)$. Because $\mu_k(T)$ of each building is generally in the range of $\overline{\mu_j}(T) \pm \overline{\sigma_{\mathrm{E},j}}(T)$, it is inferred that difference of $\mu_k(T)$ in the building group referring the same MeSO-net station is relatively small compared to the variation caused by difference between earthquake events. However, Variation of $\mu_k(T)$ in Fig. 13 is more remarkable than that in Fig. 12. One of the reasons for this variation is supposed that the buildings in Fig. 12 have relatively similar attributes to each other, whereas the two buildings in Fig. 13 differ greatly in the number of basement floors and the building scale. These differences of attributes cause the difference of the input ground motions of the buildings in Fig. 13. It suggests the necessity to consider the attributes of the building to improve the estimation accuracy of the input ground motion in the future.



 



| Attribute | |
|---|---|
| Referred MeSO-net | E.KHDM |
| No. Buildings | 10 |
| Structure | SRC:9 bldgs., RC:1 bldg. |
| Fund. Type | Pile: 8 bldgs., Spread:2 bldgs. |

| | Min. | Max. |
|---|---|---|
| No. Stories | 7 | 11 |
| No. Basement floors | 0 | 2 |
| Total floor area [sq.m] | about 2,000 | about 27,000 |

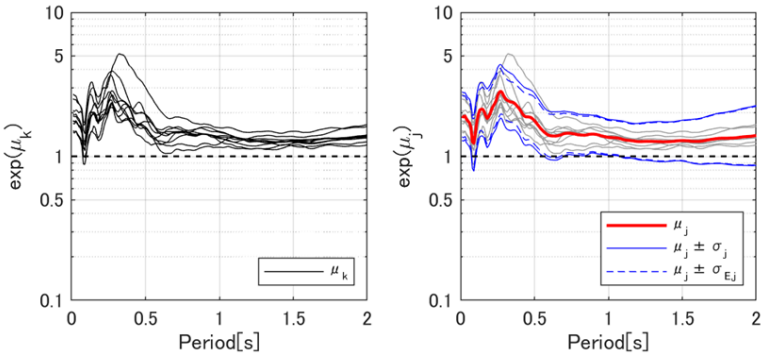


Fig. 12 – Mean acceleration response spectrum of building group (referred MeSO-net: E.KHDM)

| Attribute | |
|---|---|
| Referred MeSO-net | E.YYKM |
| No. Buildings | 2 |

| | Bldg. (A) | Bldg. (B) |
|---|---|---|
| Structure | SRC | S |
| Fund. Type | Pile | Pile |
| No. Stories | 9 | 11 |
| No. Basement floors | 1 | 5 |
| Total floor area [sq.m] | about 5,000 | about 77,000 |

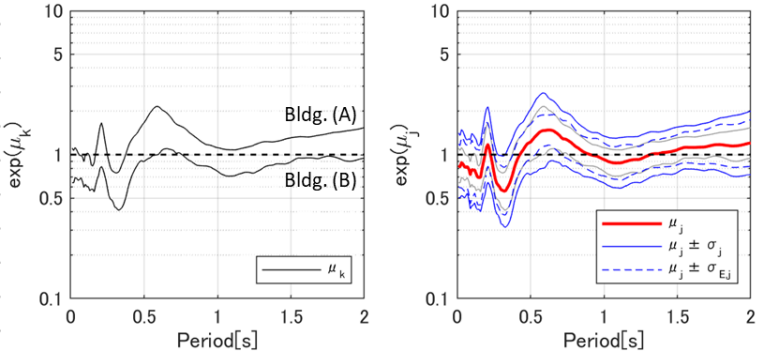


Fig. 13 – Mean acceleration response spectrum of building group (referred MeSO-net: E.YYKM)

## 6. Conclusion

In this paper, the estimation method of building input ground motions is discussed on the basis of seismic records on instrumented buildings and MeSO-net. In the analysis, 2,487 seismic records on 81 buildings are collected. The relationships between the records of the buildings and the nearest MeSO-net stations are statistically analyzed by acceleration response spectrum. The conclusions are summarized as follows:

1. The building input ground motion around individual MeSO-net station can be estimated utilizing the records on the buildings around the MeSO-net station.

2. The variation of estimated input ground motion can be decreased by utilizing the records on closer station. From this viewpoint, utilizing high dense observation array such as MeSO-net is effective for estimation of building input ground motions.

3 The acceleration response spectrum ratios of building records to MeSO-net records are suggested to be strongly influenced by the soil characteristic of referred MeSO-net station. At present, research on soil amplification characteristics at MeSO-net station is underway [6] and in future work, it may be possible to expand this estimation method to the buildings located around MeSO-net station that there is no instrumented building nearby.

## 7. Acknowledgements

This research was partially supported by the Public/Private R&D Investment Strategic Expansion PrograM (PRISM), Cabinet Office, Japan. We are grateful to the building owner for providing the observed data.



 



## 8. References

[1] Metropolitan Seismic Observation network MeSO-net, *http://www.mesonet.bosai.go.jp/mrportal/about*

[2] Kano, M., H. Nagao, K. Shiomi, R. Honda, S. Sakai, S. Nakagawa, S. Mizusako, M. Hori, and N. Hirata (2015), Azimuth verification of the MeSOnet seismographs, *Zishin, 68, 31–44*

[3] Wakamatsu, K. and Matsuoka, M. (2019), 7.5-Arc-Second Japan Engineering Geomorphologic Classification Map, *National Research Institute for Earth Science and Disaster Resilience, doi:10.17598/ NIED.0011*

[4] National Research Institute for Earth Science and Disaster Resilience (2019), NIED K-NET, KiK-net, *National Research Institute for Earth Science and Disaster Resilience, doi:10.17598/NIED.0004*

[5] Ward JH (1963), Hierarchical grouping to optimize an objective function, *Journal of the American Statistical Association, 58, 236–244*

[6] Tokyo Metropolitan Resilience Project, subproject (b), *http://forr.bosai.go.jp/sub_b/*



 